A THESIS FOR THE DEGREE OF MASTER OF SCIENCE

Estimation of Light Interception and Photosynthetic Rate of Paprika Using 3D-Scanned Plant Models and Optical Simulation According to Growth Stage and Shading Condition

3 차원 스캔 모델과 광학 시뮬레이션을 이용한 파프리카의 생육 단계 및 차광 조건별 수광과 광합성 속도 예측

BY

INHA HWANG

FEBRUARY, 2019

MAJOR IN HORTICULTURAL SCIENCE AND BIOTECHNOLOGY
DEPARTMENT OF PLANT SCIENCE
GRADUATE SCHOOL
COLLEGE OF AGRICULTURE AND LIFE SCIENCE
SEOUL NATIONAL UNIVERSITY

Estimation of Light Interception and Photosynthetic Rate of Paprika Using 3D-Scanned Plant Models and Optical Simulation According to Growth Stage and Shading Condition

UNDER THE DIRECTION OF DR. JUNG EEK SON SUBMITTED TO THE FACULTY OF THE GRADUATE SCHOOL OF SEOUL NATIONAL UNIVERSITY

BY

INHA HWANG

DEPARTMENT OF PLANT SCIENCE
SEOUL NATIONAL UNIVERSITY

FEBRUARY 2019

APPROVED AS A QUALIFIED THESIS OF INHA HWANG FOR THE DEGREE OF MASTER OF SCIENCE BY THE COMMITTEE MEMBERS

CHAIRMAN _____

KI SUN KIM, Ph.D.

VICE-CHAIRMAN _____

JUNG EEK SON, Ph.D.

MEMBER _____

HEE JAE LEE, Ph.D.

Estimation of Light Interception and Photosynthetic Rate of Paprika Using 3D-Scanned Plant Models and Optical Simulation According to Growth Stage and Shading Condition

Inha Hwang

Department of Plant Science, Graduate School of Seoul National University

ABSTRACT

In greenhouses, many crops are cultivated at high planting densities because this type of cultivation is highly productive and presents economic advantages. A high planting density causes strong mutual shading effects among adjacent crops, decreasing canopy light interception, photosynthesis, and consequently, crop yield and quality. The objective of this study was to analyze the light interception and photosynthetic rates of the paprika canopy using 3D-scanned plant models and optical simulation according to the growth stage and shading condition. Here, 3D plant models of paprika plants grown in greenhouses were constructed at 7, 35, 63, 91, and 112 days after transplanting by using a portable 3D scanner. To investigate the shading effects, the 3D-scanned plant models were arranged as isotropic forms of 1 × 1, 3 × 3, 5 × 5, 7 × 7, and 9 × 9 plants with a distance of 60 cm between plants, and the light interception of the center

plant in the arrangement was obtained with the growth stage by simulation. The canopy photosynthetic rates were calculated using the Farquhar, von Caemmerer, and Berry (FvCB) model. The total canopy light interception and light interception per unit leaf area of the center plant decreased due to the self- and mutual shading effects caused by the growth of each plant and the increase in the number of surrounding plants. The canopy photosynthetic rates showed similar patterns to those of the total light interception, but their decreasing rate was less than that of the total light interception because the leaf photosynthetic rate was saturated at the top of the canopy. In this study, the spatial distributions of the canopy light interception and photosynthetic rates could be analyzed by using 3D-scanned models of paprika and optical simulation. This method can be an effective tool for designing crop cultivation systems as well as estimating canopy light interception and photosynthesis in greenhouses.

Keywords: Canopy, Light distribution, Mutual shading, Ray-tracing, Self-shading

Student number: 2017-28139

CONTENTS

LIST OF TABLES

LIST OF FIGURES

INTRODUCTION

In greenhouses, many crop species were cultivated at high planting densities given economic advantages of high productivity. However, a high planting density causes strong mutual shading effects among adjacent plants, decreasing canopy light interception (Chen et al., 1999). As a result, vegetative growth of crops is restricted, and the fruit quality also decreases (Aminifard et al., 2012). The decreased light interception of lower leaves due to shading causes reduced net photosynthesis in the entire crop canopy (Tanaka and Kawano, 1966). Since crop yield is determined by accumulated products from canopy photosynthesis driven by canopy light interception (Monteith, 1965), planting density has been optimized to maximize canopy light interception and crop yield in greenhouses (Tanaka and Kawano, 1966; Anten et al., 1995; Goudriaan, 1995).

However, optimal planting densities have been provided by indirect parameters, such as leaf area density or number of plants per m^2. In actual cultivation conditions, canopy light interception and photosynthesis are mainly determined by light environment factors in greenhouses, such as meteorological factors and greenhouse structures. Morphological and structural characteristics of crops affected the canopy photosynthesis (Caldwell et al., 1986; Kim et al., 2016). Therefore, light distribution and leaf photosynthesis of crops must be accurately estimated to analyze the canopy photosynthesis (Chen at al., 2015).

Three-dimensional virtual plant models have been introduced for analyzing canopy light interception with more complicated but accurate computational approaches. Given advancements in 3D graphic technology, plant architecture can be expressed by computer graphic tools (Smith, 1984; Prusinkiewicz, 1986). By constructing 3D-structured plant models and performing an optical simulation, spatial light distributions can be accurately estimated even on irregular plants and canopy structures, and canopy photosynthesis can be more accurately calculated with the obtained light distribution (Buck-Sorlin et al., 2011; Sarlikioti et al., 2011; De Visser et al., 2014; Kim et al., 2016; Jung et al., 2018).

The estimation accuracy depends on the accuracy of the reconstructed 3D plant models. However, existing 3D plant models do not reflect exact structures of the actual plant because plant organs, such as leaf, stem, and fruit, are represented as simplified features. Three-dimensional-scanning technology can be an appropriate solution to this problem by precisely scanning the structure and surface of actual plants (Paulus et al., 2014; Zhang et al., 2016). Although several studies on 3D-scanned plant models have been published, they were mainly focused on the precise reconstruction of plant structures (Hosoi et al., 2011; Wahabzada et al., 2015; Behmann et al., 2016; Moriondo et al., 2016). The objective of this study is to analyze the light interception and photosynthetic rate of paprika canopy using 3D-scanned plant models and optical simulation according to growth stage and shading condition.

LITERATURE REVIEW

Mutual Shading and Optimal Planting Density

In greenhouses, many crop species are cultivated at high planting densities because of economic advantages of high productivity (Thornley, 1983). At a high planting density, strong mutual shadings occur among adjacent plants, reducing photosynthetic capacities such as nitrogen content and chlorophyll a/b ratio of shaded lower leaves (Pearcy, 1998; Dinç et al., 2012; Li et al., 2014). However, the respiration of entire canopy proceeds as upper leaves, leading the loss of net photosynthesis (Tanaka and Kawano, 1966). Carbohydrate accumulation and bud growth are inhibited due to the decreased light transmission (Foster et al., 1993). Competition among crops can occur for nutrients, physical spaces, and moisture at high planting densities (Law-Ogbomo and Egharevba, 2009). Modeling approaches have been conducted to find optimal planting densities for maximizing dry matter productions, and to determine optimal leaf area index (LAI) with different daily irradiation and canopy nitrogen levels (Anten et al., 1995; Goudriaan, 1995).

Development of Process-Based Plant Models

The first-developed plant models were process-based models (PBMs), which explain the crop growth with a set of mathematical equations. In PBMs,

crops were divided into organs such as leaves, stems, roots and reproductive or storage organs (Marcelis et al., 1998). PBMs calculated the crop growth with a flow of dry matter, and its production started from the light interception by LAI (Van Ittersum et al., 2003). Light interception of crop canopy was calculated with an assumption that the light intensity is exponentially decreasing from the top to the bottom of crop canopy (Monsi and Saeki, 1953). This assumption exhibited a practical simplicity and reliable accuracy with variables of extinction coefficient k and overlying LAI. Gross photosynthesis was calculated by a simple equation with maximum rate of leaf photosynthesis and a rectangular hyperbola curve (Thornley 1976; Goudriaan et al., 1995). Whole canopy photosynthetic rate is calculated by summing individual leaf photosynthetic rate. Later, the Farquhar, von Caemmerer, and Berry (FvCB) model has widely been adapted and expressed the leaf photosynthetic rate with various environmental factors such as activity of Ribulose-1,5-bisphosphate carboxylase/oxygenase (Rubisco) and Ribulose 1,5-bisphosphate (RuBP), temperature, intercellular CO_2 concentration, and absorbed irradiation (Farquhar et al., 1980).

Development of Functional Structural Plant Models

The next generation model called ‘architectural model’ is based on the ‘L-systems’ which explain the development of multicellular organism by

describing the shape, position, and properties of the (n+1)–th element as functions of those of the n–th element (Lindenmayer, 1968a, b). With an advancement of computer graphics, plant architectures can be expressed on 3D space (Smith, 1984; Prusinkiewicz, 1986). In the architectural model, plants were treated as closed cybernetic systems, meaning that there was no interaction between plant development and environment (Vos et al., 2007). With the development of functional-structural plant models (FSPMs) (Sievänen et al., 2000; Godin and Sinoquet, 2005) or virtual plant models (Room et al., 1996; Hanan, 1997), development of 3D plant architectures over time can be reflected. Therefore, FSPMs enabled to model the material flow within the 3D plant model and environment (Vos et al., 2007). Light distributions on the 3D plant canopy can be obtained by ray-tracing simulation (Cieslak et al., 2008; Buck-Sorlin et al., 2009; Sarlikioti et al., 2011; Henke, 2018). By using canopy photosynthetic properties, canopy photosynthetic rates could be more accurately calculated (Buck-Sorlin et al., 2011; De Visser et al., 2014; Kim et al., 2016; Jung et al., 2018). 3D scanning technology has been adopted to 3D plant modelling with high accuracy in representing the structure and surface of actual plants (Paulus et al., 2014; Zhang et al., 2016). Precise construction and extraction of plant structures were conducted by using the 3D-scanned plant models (Hosoi et al., 2011; Wahabzada et al., 2015; Jan Behmann et al., 2016; Moriondo et al., 2016).

MATERIALS AND METHODS

Plant Materials and Cultivation Conditions

This experiment was conducted in Venlo-type greenhouses of the Protected Horticulture Research Institute, National Institute of Horticultural and Herbal Sciences (RDA), Haman, Korea (35.2°N, 128.4°E). Paprika plants (*Capsicum annuum* L. 'Scirocco') were sown on a tray on February 8, 2018 and transferred on cubes on March 5, 2018. After raising seedlings, the plants were transplanted on the slabs with a planting density of two plants·m^{-2} on April 6, 2018. The four cubes were planted on each slab. During the seedling period, electrical conductivity (EC) of nutrient solutions was 0.8 dS·m^{-1}. The EC was gradually increased by 0.2 dS·m^{-1} every week and maintained at 2.5 dS·m^{-1} at the last seedling stage. After the transplanting, the nutrient solutions with EC 2.5 dS·m^{-1} and pH 6.0 were supplied 14 times a day at 33 mL per plant by drip irrigation.

3D Scanning and Reconstruction of 3D Plant Models

Three-dimensional scanning of the plants was performed with a portable 3D scanner (GO!SCAN50™, CREAFORM, Lévis, Quebec, Canada) at 7, 35, 63, 91, and 112 days after transplanting (DAT). To improve the accuracy of the 3D-scanned results, a circular target with a diameter of 10 mm was attached to the surface of leaves, stems and fruits of the plants. Three-dimensional scanning

was performed with a resolution of 2 mm. The 3D-scanned mesh obtained by 3D scanning was transformed into a parametric model using scanning software (Vxelement, CREAFORM, Lévis, Quebec, Canada) and reverse engineering software (Geomagic Design X, 3D Systems, Rock Hill, SC, USA) and reconstructed in a 3D CAD software (SOLIDWORKS, Dassault Systèmes, Vélizy-Villacoublay, France). To apply the optical properties of the plants to the 3D plant model, the transmittance (*Tr*) and reflectance (*Ref*) of the plant leaves were measured with an integrating sphere combined with a spectroradiometer in the range of 400-700 nm. Absorption (*Abs*) of leaves was calculated with equations as $Abs = 1 - (Tr + Ref)$. The measurement was conducted with three randomly sampled leaves each from the top, middle, and lower portions of the plant canopy.

Arrangement of Surrounding Plants and Optical Simulation

For investigating the shading effect of surrounding plants, the 3D-scanned plant models were arranged as isotropic forms of 1 × 1, 3 × 3, 5 × 5, 7 × 7, and 9 × 9 plants. The spatial light distribution of the 3D plant located in the center was obtained by optical simulation (OPTISWORKS, OPTIS Inc., La Farlède, FRANCE) (Fig. 1). The distance between the plants were decided as 60 cm to avoid the overlapping of leaves. Three-dimensional plant models at 7, 35, 63, 91, and 112 DAT were used. As optical simulation conditions, the location and date were set to equator (0.0°N, 0.0°E) and April 26, 2018, respectively.

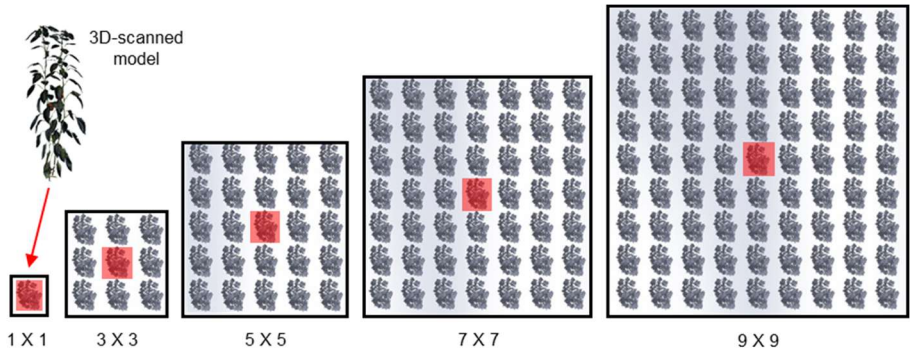

Fig. 1. Isotropic arrangements of 1 × 1, 3 × 3, 5 × 5, 7 × 7, and 9 × 9 paprika plants with a distance of 60 cm between the plants. A plant located in the center (red-colored) is the target plant to be analyzed.

The time was set to noon. At that time, the solar zenith angle was 76.4°. The number of rays used in the optical simulation was set to 100 mega-rays. The atmospheric turbidity was set to 3, which means a general clear sky with a visible distance of 10 km. The ratio of direct and scattered light was 6:4. For verification of optical simulation, daily light intensities in a greenhouse (35.2°N, 128.4°E; Haman, Korea on July 4, 2018) measured using a quantum sensor (SQ-110, Apogee Instrument Inc., Logan, Utah, USA) were compared with simulated values and showed good agreements (Fig. A1).

Calculation of photosynthetic rate

Photosynthetic rates were calculated by the FvCB model as follows:

$$P = \min(A_c, A_j) - R \quad \text{(Eq. 1)}$$

$$A_c = \left(\frac{V_c(C_i - \Gamma^*)}{C_i + K_c(1 + \frac{O}{K_o})}\right) \quad \text{(Eq. 2)}$$

$$V_c = V_{cmax}\left(\frac{31 + (\frac{69}{1 + e^{-0.009(PAR - 500)}})}{100}\right) \quad \text{(Eq. 3)}$$

$$A_j = \left(\frac{J(C_i - \Gamma^*)}{4C_i + 8\Gamma^*}\right) \quad \text{(Eq. 4)}$$

$$J = \left(\frac{\alpha PAR + J_{max} - \sqrt{(\alpha PAR + J_{\max})^2 - 4\theta J_{\max}\alpha PAR}}{2\theta}\right) \quad \text{(Eq. 5)}$$

where P is leaf net assimilation rate (μmol $CO_2 \cdot m^{-2} \cdot s^{-1}$); A_c and A_j are leaf gross assimilation rates limited by Rubisco activity (μmol $CO_2 \cdot m^{-2} \cdot s^{-1}$) and RuBP regeneration (μmol $CO_2 \cdot m^{-2} \cdot s^{-1}$), respectively; R is non-photorespiratory

respiration rate (μmol $CO_2 \cdot m^{-2} \cdot s^{-1}$); V_c is carboxylation capacity at specific light intensity (μmol $CO_2 \cdot m^{-2} \cdot s^{-1}$); C_i is intercellular CO_2 concentration (μmol·mol^{-1}); Γ^* is CO_2 compensation point (μmol·mol^{-1}); K_c and K_o are Michaelis–Menten constants of Rubisco for CO_2 and O_2 (μmol·mol^{-1}), respectively; O is oxygen concentration (μmol·mol^{-1}); PAR is photosynthetic photon flux density (PPFD, μmol·$m^{-2} \cdot s^{-1}$); α is efficiency of light energy conversion on an incident light (mol·mol^{-1}); J_{max} is maximum electron transport rate (μmol $CO_2 \cdot m^{-2} \cdot s^{-1}$); and θ is curvature of light response of J (dimensionless) (Qian et al., 2012). Air temperature, relative humidity, and CO_2 concentration were assumed as 27°C, 60%, and 400 mol·mol^{-1}, respectively. V_{cmax} and J_{max} values of top, middle, and bottom leaf positions in paprika plant were obtained as 81.9, 37.0, and 14.6, and 162.4, 38.4, and 12.3, respectively (Table 1).

Table 1. Maximum electron transport rate (J_{max}), maximum carboxylation capacity (V_{cmax}), and respiration (R) of paprika plants in the FvCB model according to leaf position.

Leaf position	J_{max}	V_{cmax}	R
Top	81.9	162.4	-1.2
Middle	37.0	38.4	-0.4
Bottom	14.6	12.3	-0.3

RESULTS

Construction of 3D Plant Models with Growth Stage

Paprika plant models at DAT 7, 35, 63, 91, and 112 were constructed by 3D scanning (Fig. 2). For each growth stage, the plant heights were 61.4, 89.8, 119.5, and 170.2 cm; the number of leaves were 13, 31, 51, 64, and 79; and the total leaf areas were 0.10, 0.37, 0.66, 0.85, and 1.13 m^2, respectively (Table A1).

Spatial Canopy Light Interception with Number of Surrounding Plants and Growth Stage

The optical simulation with isotropic arrangements of 3D-scanned paprika models showed that the light interception was highest at the top of the canopy and decreased to the bottom (Fig. 3). As the number of surrounding plants increased, the amount of intercepted lights of the center plant tended to decrease and finally converged to constant values in all growth stages (Fig. 4). In particular, the light interception of the plants at 112 DAT was greatly decreased due to the mutual shading of the surrounding plants (Fig. 4). At 1 × 1 (without surrounding plants), the canopy light interception was increased to 29.1, 86.8, 164.3, 209.2, and 237.9 $J \cdot s^{-1}$ at 7, 35, 63, 91, and 112 DAT. At early growth stage (7 DAT), the canopy light interception was 29.1 $J \cdot s^{-1}$ at 1 × 1,

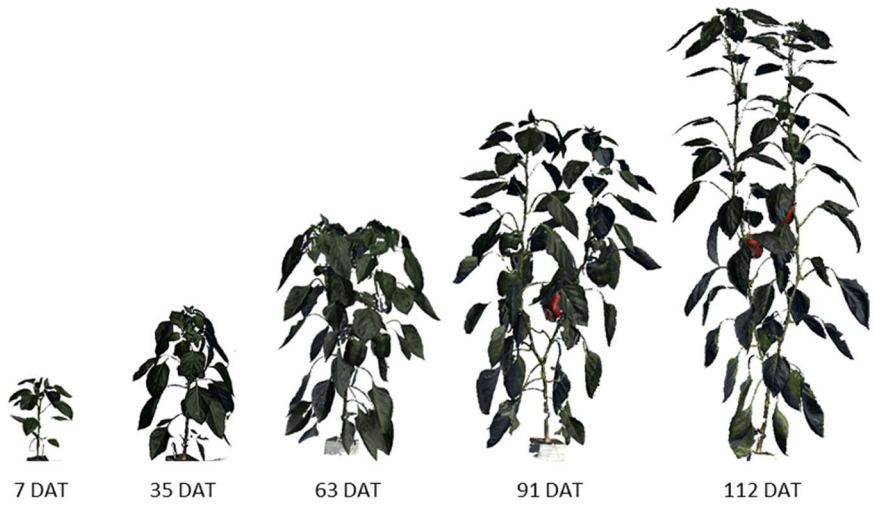

Fig. 2. 3D plant models of paprika plants grown in greenhouses scanned at 7, 35, 63, 91, and 112 days after transplanting (DAT).

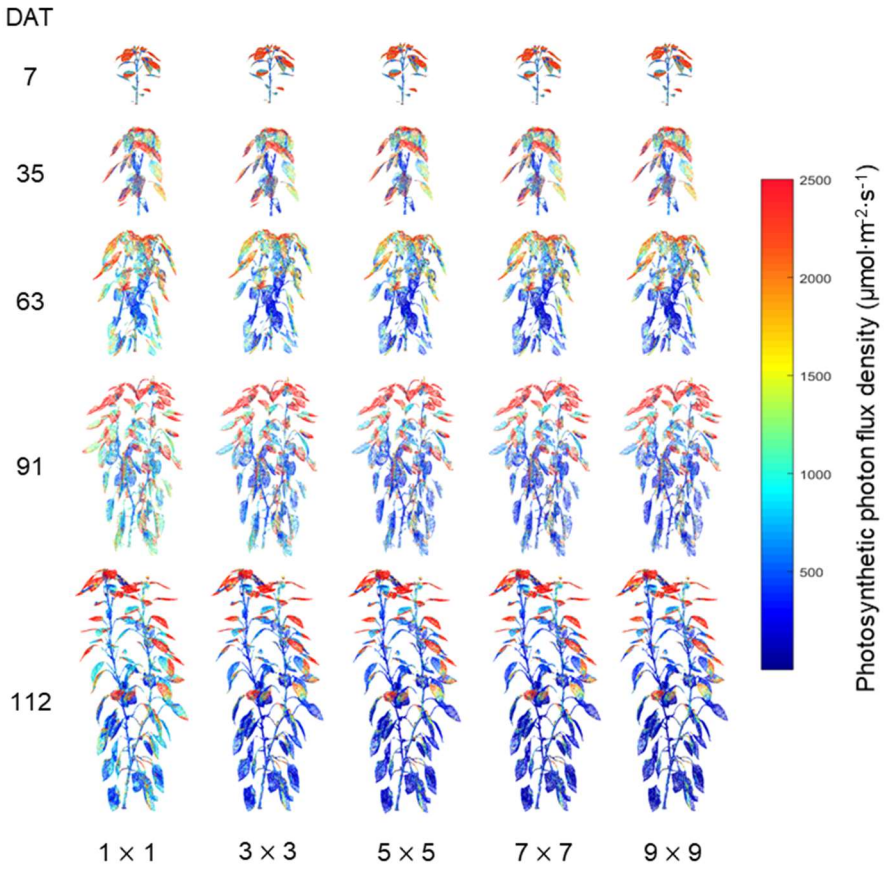

Fig. 3. Spatial distribution of light interceptions of 3D-scanned paprika models at isotropic arrangements of 1 × 1, 3 × 3, 5 × 5, 7 × 7, and 9 × 9 plants at 7, 35, 63, 91, and 112 days after transplanting (DAT).

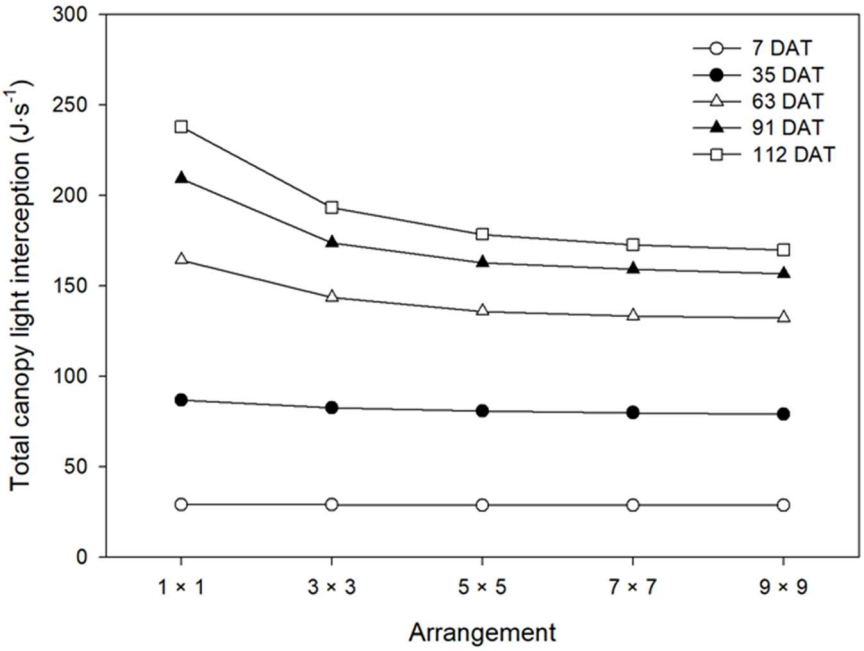

Fig. 4. Changes in total canopy light interception of 3D-scanned paprika models with increasing number of surrounding plants at 7, 35, 63, 91, and 112 days after transplanting (DAT). Refer to Fig. 1 for 1 × 1, 3 × 3, 5 × 5, 7 × 7, and 9 × 9 isotropic arrangements of surrounding plants.

and 28.5 $J \cdot s^{-1}$ at 9 × 9, showing a reduction of 2.0%. As the growth progressed to 35, 63, 91, and 112 DAT, the light interceptions in the plant at 9 × 9 considerably decreased by 9.0, 19.5, 25.2, and 28.6% compared with those in the plant at 1 × 1.

The vertical light distribution of the plant at 112 DAT was calculated using the spatial light distribution by optical simulation (Fig. 5A). At 1 × 1, the average light interception of the top canopy was 1,831.5 $\mu mol \cdot m^{-2} \cdot s^{-1}$, while it decreased to 1,176.5 $\mu mol \cdot m^{-2} \cdot s^{-1}$ at the bottom. At 9 × 9, the average light interception of upper canopy was similar to that at 1 × 1 with 1,747.6 $\mu mol \cdot m^{-2} \cdot s^{-1}$, but it sharply deceased at approximately 110 cm height and showed 681.4 $\mu mol \cdot m^{-2} \cdot s^{-1}$ at the bottom. The difference in average light interception between the two arrangements was approximately 100 $\mu mol \cdot m^{-2} \cdot s^{-1}$ at a plant height greater than 110 cm (Fig. 5B), while it became larger at a plant height less than 110 cm. The highest value was noted at 110 cm with 719.5 $\mu mol \cdot m^{-2} \cdot s^{-1}$ (Fig. 5B).

Spatial Canopy Photosynthetic Rate Based on Number of Surrounding Plants and Growth Stage

Photosynthetic rate was highest at the top of the canopy and decreased to the bottom at all growth stages (Fig. 6). As the number of surrounding plants increased, the canopy photosynthetic rate of the plant in the center tended to

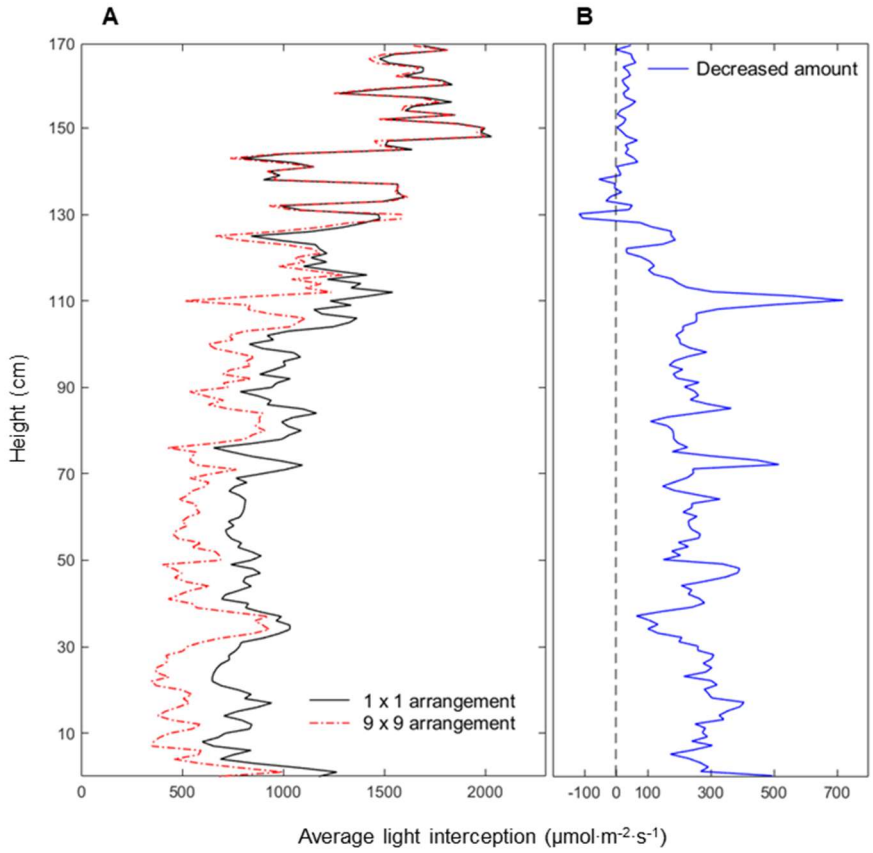

Fig. 5. Vertical analyses of average light interception (A) and decreased amount of the light interception (B) of 3D-scanned paprika models at isotropic arrangements of 1 × 1 and 9 × 9 plants at 112 days after transplanting.

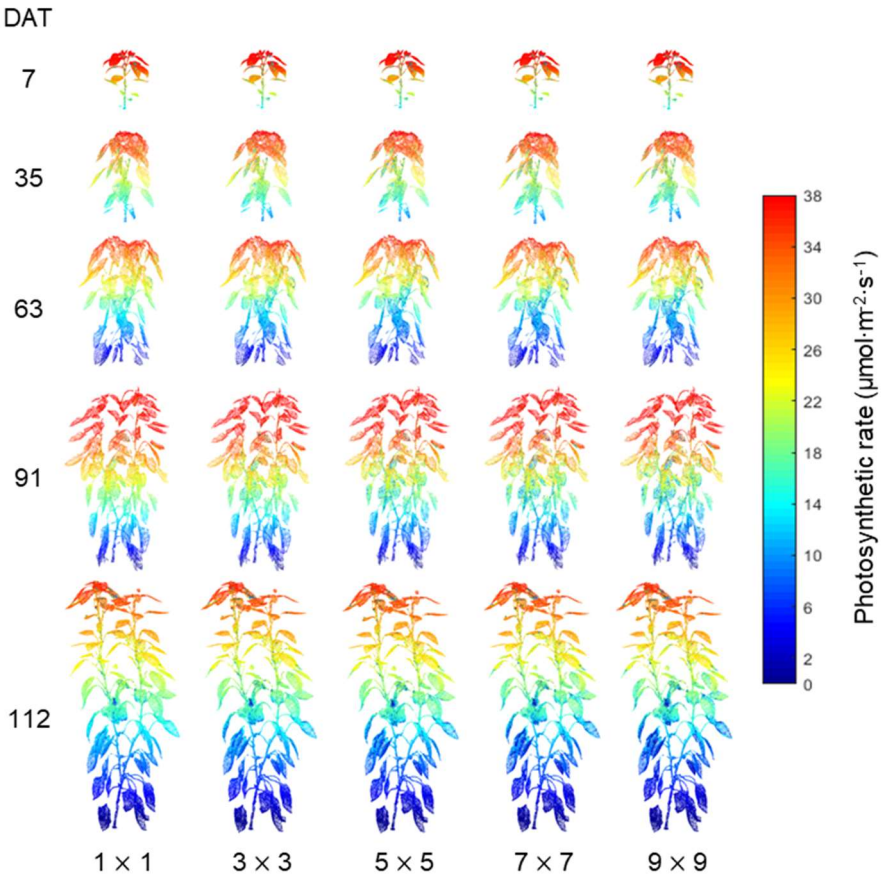

Fig. 6. Spatial distribution of photosynthetic rates of 3D-scanned paprika models at isotropic arrangements of 1 × 1, 3 × 3, 5 × 5, 7 × 7, and 9 × 9 plants at 7, 35, 63, 91, and 112 days after transplanting (DAT).

decrease and finally converged (Fig. 7). In particular, the plants at 112 DAT showed great decrease in canopy photosynthetic rate due to the shading of the surrounding plants. At 1 × 1, the canopy photosynthetic rate increased to 2.60, 7.23, 13.61, 16.38, and 23.93 $g \cdot h^{-1}$ at 7, 35, 63, 91, and 112 DAT, respectively. At early growth stage (7 DAT), the canopy photosynthetic rate was 2.60 $g \cdot h^{-1}$ at 1 × 1, and 2.57 $g \cdot h^{-1}$ at 9 × 9, showing a reduction of 1.20%. However, as the growth progressed to 35, 63, 91, and 112 DAT, the canopy photosynthetic rate in the plant at 9 × 9 considerably decreased by 5.4, 8.2, 11.6, and 15.6% compared with those in the plant at 1 × 1.

Effects of Self- and Mutual Shadings on Canopy Light Interception and Photosynthetic Rate

While the canopy light interception and canopy photosynthetic rate of the plants increased with growth stage, those per unit leaf area showed opposite results (Tables 2, 3). The light interception per unit leaf area was highest at 1 × 1 at DAT 7 with 324.4 $J \cdot s^{-1} \cdot m^{-2}$ and tended to decrease as the plants grew. As the number of surrounding plants increased, the intercepted light per unit leaf area also decreased. The light interception per unit leaf area according to growth stage and number of surrounding plants decreased from 82.8% at 35 DAT to 56.0% at 112 DAT compared to the plant at 7 DAT at 1 × 1 (Table 2). At 9 × 9, the light interception per unit leaf area decreased to 98.0% at 7 DAT to 40.0% at 112 DAT compared with those of 7 DAT at 1×1.

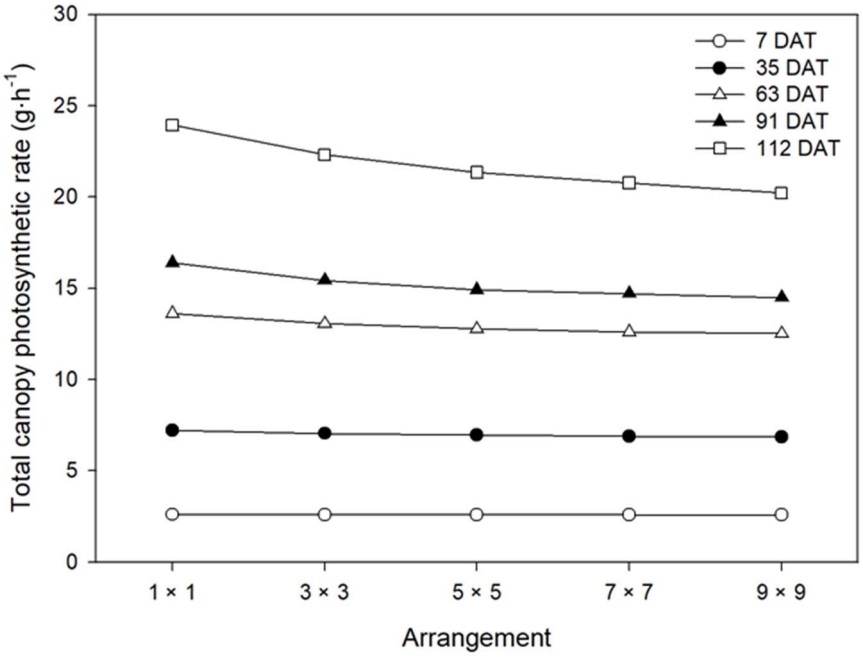

Fig. 7. Changes in total canopy photosynthetic rate of 3D-scanned paprika models with increasing number of surrounding plants at 7, 35, 63, 91, and 112 days after transplanting (DAT). Refer to Fig. 1 for 1 × 1, 3 × 3, 5 × 5, 7 × 7, and 9 × 9 isotropic arrangements of surrounding plants.

Table 2. Decreasing rate of light interception per unit leaf area of 3D paprika models with increasing number of surrounding plants at 7, 35, 63, 91, and 112 days after transplanting (DAT). Refer to Fig. 1 for 1 × 1, 3 × 3, 5 × 5, 7 × 7, and 9 × 9 isotropic arrangements of surrounding plants.

Growth stage (DAT)	Rate of light interception per unit leaf area				
	1 × 1	3 × 3	5 × 5	7 × 7	9 × 9
7	1.000[z]	0.994	0.986	0.982	0.980
35	0.828	0.787	0.770	0.762	0.754
63	0.763	0.667	0.631	0.619	0.614
91	0.718	0.597	0.559	0.547	0.538
112	0.560	0.455	0.420	0.407	0.400

[z]Canopy light interception per leaf area = 324.4 $J \cdot s^{-1} \cdot m^{-2}$

Table 3. Decreasing rate of photosynthetic rate per unit leaf area of 3D paprika models with increasing number of surrounding plants at 7, 35, 63, 91, and 112 days after transplanting (DAT). Refer to Fig. 1 for 1 × 1, 3 × 3, 5 × 5, 7 × 7, and 9 × 9 isotropic arrangements of surrounding plants.

Growth stage (DAT)	Rate of photosynthetic rate per unit leaf area				
	1 × 1	3 × 3	5 × 5	7 × 7	9 × 9
7	1.000[z]	0.998	0.994	0.993	0.988
35	0.771	0.753	0.742	0.736	0.731
63	0.707	0.679	0.663	0.655	0.650
91	0.630	0.593	0.573	0.565	0.557
112	0.631	0.588	0.563	0.547	0.533

[z]Canopy photosynthetic rate per leaf area = 28.98 $g \cdot m^{-2} \cdot h^{-1}$

Similarly, the photosynthetic rate per unit leaf area was highest at 1 × 1 at 7 DAT with 324.4 $J \cdot s^{-1} \cdot m^{-2}$ and showed a similar trend to the light interception per unit leaf area (Table 3). As the number of surrounding plants increased, the photosynthetic rate per unit leaf area also decreased. The photosynthetic rate per unit leaf area according to growth stage and number of surrounding plants decreased from 77.1 at 35 DAT to 63.1% at 112 DAT compared with the plant at 7 DAT at 1 × 1 (Table 3). At 9 × 9, the photosynthetic rate per unit leaf area decreased to 98.8% at 7 DAT to 53.8% at 112 DAT compared with those of 7 DAT at 1×1.

DISCUSSION

The light interception per unit leaf area of the center plant in the arrangement of surrounding plants showed different change patterns with growth stage from the canopy light interception. However, both the canopy light interception and light interception per unit leaf area tended to decrease with increasing number of surrounding plants (Figs. 3, 4, Table 2). This finding is due to the self- and mutual shading effects caused by the growth of each plant and the increase in the number of surrounding plants (Tanaka and Kawano, 1966). Shadings occur not only between adjacent plants as mutual shading but also can occur within an individual plant canopy as self-shading (Hilker et al., 2008; Marchiori et al., 2014). Through the optical simulation, both shading effects could be analyzed (Figs. 3, 5A, 5B). At a solar altitude in the simulation condition, the shading distance, which is the minimum planting distance through which the plants can completely receive the direct sunlight, was calculated as 41.2 cm at 112 DAT (Table A2). Because the distance between plant models was set to 60 cm in this study, the reduced light interception with increasing number of surrounding plants occurred by the shading of diffused lights. Thus, the light interception of the entire crop canopy is reduced due to the interception of the diffused light by surrounding plants, particularly, causing larger decrease in light intensity at the middle and bottom parts of the canopy

(Utsugi, 1999; Suzaki et al., 2003; Fig. 5B). In Korea, the solar altitude in the summer season is approximately 70^{o} which is considerably reduced to approximately 30^{o} in the winter season (Kim and Park, 2010; Kim and Lee, 2011). Therefore, in the winter season with low solar altitude, the shading distance is longer than summer season, indicating that the mutual shading caused by surrounding plants increases.

The photosynthetic distribution and photosynthetic rate calculated by the FvCB model showed similar trends to the change in the total canopy light interception. On the other hand, the decreasing rate of canopy photosynthetic rate was smaller than those of the total light interception affected by the growth stage and the number of surrounding plants (Fig. 7). The photosynthetic rate per unit leaf area also showed a smaller decrease compared with the light interception per unit leaf area (Table 3). This finding is probably due to the environmental conditions of the simulation. In this study, the atmospheric CO_2 concentration was assumed to be 400 μmol·mol^{-1}, which is the average atmospheric CO_2 concentration. At 400 μmol·mol^{-1} CO_2, the photosynthetic rate of the top leaves of the canopy was saturated with 36.7 μmol CO_2·m^{-2}·s^{-1} when PPFD was 2,500 μmol CO_2·m^{-2}·s^{-1}. In Korea, daily solar radiation is highly variable. Particularly in summer, PPFD in greenhouses increases to greater than 2,000 μmol CO_2·m^{-2}·s^{-1} (Shin et al., 2014). Therefore, CO_2 is enriched to increase the photosynthetic capacity of the crops in greenhouses. Many results showed that the photosynthetic rates increased by enriched CO_2

in various crops, such as tomato, cucumber, and sweet pepper (Wittwer and Robb, 1964; Nederhoff and Vegter, 1994; Körner et al., 2007). Thus, analysis of canopy photosynthetic rate using 3D plant model and optical simulation could be helpful in establishing CO_2 fertilization strategies in greenhouses (Son et al., 1999; Hu et al., 2011; Jung et al., 2016).

Given the shading effect, the photosynthetic activity of the shaded lower leaves is limited by lower light intensity, but respiration proceeds as the upper leaves, decreasing nitrogen content and chlorophyll a/b ratio (Pearcy 1998; Dinç et al., 2012; Li et al., 2014), reducing photosynthetic function and subsequent loss in net canopy photosynthesis (Tanaka and Kawano, 1966). Crops cultivated at lower planting densities are reported to be more vigorous than those at higher planting densities, and the fruit qualities, such as fruit weight, volume and vitamin C content were also improved (Aminifard et al., 2012). However, the yield per plant is higher at lower planting densities, while the yield per unit area increased at higher planting densities due to the increase in the number of plants per unit area (Thornley, 1983; Aminifard et al., 2010). Thus, most greenhouse crops are cultivated at high planting densities inhibiting photosynthate accumulation and bud growth due to the decreased light transmission (Foster et al., 1993). Moreover, at higher planting densities, competition for nutrients, physical spaces, and moisture among crops can occur (Law-Ogbomo and Egharevba, 2009). This study suggested the possibility of presenting optimal cultivation conditions by analyzing shading effects

according to growth stage and planting density by using 3D plant model and optical simulation.

CONCLUSION

The light interception and photosynthetic rate of paprika canopy was analyzed by using 3D-scanned paprika models and optical simulation at different growth stage and shading conditions. The canopy light interception and light interception per unit leaf area decreased due to the self- and mutual shading effects caused by the growth of each plant and the increased number of surrounding plants. The canopy photosynthetic rate showed a similar decreasing pattern to the light interception but the decrease considerably smaller due to the saturation of leaf photosynthetic rate of the plants. This method could be effective for designing cultivation systems as well as predicting canopy light interception and photosynthetic rate in greenhouses.

LITERATURE CITED

Aminifard MH, Aroiee H, Ameri A, Fatemi H (2012) Effect of plant density and nitrogen fertilizer on growth, yield, and fruit quality of sweet pepper (*Capsicum annum* L.). Afr J Agr Res 7:859–866

Aminifard MH, Arouiee H, Karimpour S, Neamati SH (2010) Growth and yield characteristics of paprika pepper (*Capsicum annum* L.) in response to plant density. Asian J Plant Sci 9:276–280

Anten NPR, Schieving F, Medina E, Werger MJA, Schuffelen P (1995) Optimal leaf area indices in C3 and C4 mono- and dicotyledonous species at low and high nitrogen availability. Physiol Plant 95:541–550

Behmann J, Mahlein AK, Paulus S, Dupuis J, Kuhlmann H, Oerke EC, Plümer L (2016) Generation and application of hyperspectral 3D plant models: Methods and challenges. Mach Vision Appl 27:611–624

Buck-Sorlin GH, de Visser PHB, Henke M, Sarlikioti V, van der Heijden GWAM, Marcelis LFM, Vos J (2011) Towards a functional-structural plant model of cut-rose: Simulation of light environment, light absorption, photosynthesis, and interference with the plant structure. Ann Bot 108:1121–1134

Buck-Sorlin GH, Hemmerling R, Vos J, de Visser PHB (2009) Modelling of spatial light distribution in the greenhouse: Description of the model. 3rd Intl Symp Plant Growth Model Sim Vis App, Beijing, China pp 79–86

Caldwell MM, Meister HP, Tenhunen JD, Lange OL (1986) Canopy structure, light microclimate, and leaf gas exchange of *Quercus coccifera* L. in a Portuguese macchia: Measurements in different canopy layers and simulations with a canopy model. Trees 1:25–41

Chen JM, Liu J, Cihlar J, Goulden ML (1999) Daily canopy photosynthesis model through temporal and spatial scaling for remote sensing applications. Ecol Model 124:99–119

Chen TW, Nguyen TM, Kahlen K, Stützel H (2015) High temperature and vapor pressure deficit aggravate architectural effects but ameliorate non-architectural effects of salinity on dry mass production of tomato. Front Plant Sci 6:887

Cieslak M, Lemieux C, Hanan J, Prusinkiewicz P (2008) Quasi-Monte Carlo simulation of the light environment of plants. Funct Plant Biol 35:837–849

De Visser PHB, Buck-Sorlin GH, van der Heijden GWAM (2014) Optimizing illumination in the greenhouse using a 3D model of tomato and a ray tracer. Front Plant Sci 5:48

Dinç E, Ceppi MG, Tóth SZ, Bottka S, Schansker G (2012) The chl *a* fluorescence intensity is remarkably insensitive to changes in the chlorophyll content of the leaf as long as the chl *a/b* ratio remains unaffected. Biochim Biophys Acta Bioenerg 1817:770–779

Farquhar GD, von Caemmerer S, Berry JA (1980) A biochemical model of photosynthetic CO_2 assimilation in leaves of C3 species. Planta 149:78–90

Foster M, Kleine G, Moore J, Janick J, Simon JE (1993) Impact of seeding rate and planting date on guayule stand establishment by direct seeding in West Texas. New Crops, pp 354–355

Godin C, Sinoquet H (2005) Functional-structural plant modelling. New Phytol 166:705–708

Goudriaan J (1995) Optimization of nitrogen distribution and leaf area index for maximum canopy assimilation rate. Nitrogen Management Studies in Irrigated Rice, pp 85–97

Hanan J (1997) Virtual plants-integrating architectural and physiological models. Environ Modell Softw 12:35–42

Henke M, Buck-Sorlin GH (2018) Using a full spectral ray-tracer for calculating light microclimate in functional-structural plant modelling. Comput Inform 36:1492–1522

Hilker T, Coops NC, Schwalm CR, Jassal RPS, Black TA, Krishnan P (2008) Effects of mutual shading of tree crowns on prediction of photosynthetic light-use efficiency in a coastal Douglas-fir forest. Tree Physiol 28:825–834

Hosoi F, Nakabayashi K, Omasa K (2011) 3-D modeling of tomato canopies using a high-resolution portable scanning lidar for extracting structural information. Sensors 11:2166–2174

Hu E, Tong L, Hu D, Liu H (2011) Mixed effects of CO_2 concentration on photosynthesis of lettuce in a closed artificial ecosystem. Ecol Eng 37:2082–2086

Jung DH, Kim D, Yoon HI, Moon TW, Park KS, Son JE (2016) Modelling the canopy photosynthetic rate of romaine lettuce (*Lactuca sativa* L.) grown in a plant factory at varying CO_2 concentrations and growth stages. Hortic Environ Biotechnol 57:487–492

Jung DH, Lee JW, Kang WH, Hwang IH, Son JE (2018) Estimation of whole plant photosynthetic rate of Irwin mango under artificial and natural lights using a three-dimensional plant model and ray-tracing. Intl J Mol Sci 19:152

Kim DW, Park CS (2010) Energy performance assessment of a double skin system for various configurations. J Architec Inst Kor Struct Constr 26:379–387

Kim JH, Lee JW, Ahn TI, Shin JH, Park KS, Son JE (2016) Sweet pepper (*Capsicum annuum* L.) canopy photosynthesis modelling using 3D plant architecture and light ray-tracing. Front Plant Sci 7:1321

Kim SY, Lee JH (2011) The influence of photosensor configurations on control performance of daylight dimming systems in a small private office. Kor J Air Cond Refrig Eng 23:231–242

Körner, Oliver A, Van't Ooster, Hulsbos M (2007) Design and performance of a measuring system for CO_2 exchange of a greenhouse crop at different light levels. Biosyst Eng 97:219–228

Law-Ogbomo KE, Egharevba RKA (2009) Effects of planting density and

NPK fertilizer application on yield and yield components of tomato (*Lycospersicon esculentum* Mill.) in forest location. World J Agric Sci 5:152–158

Li T, Liu LN, Jiang CD, Liu YJ, Shi L (2014) Effects of mutual shading on the regulation of photosynthesis in field-grown sorghum. J Photochem Photobiol B Biol 137:31–38

Lindenmayer A (1968a) Mathematical models for cellular interactions in development. I. Filaments with one-sided inputs. J Theor Biol 18:280–299

Lindenmayer A (1968b) Mathematical models for cellular interactions in development. II. Simple and branching filaments with two-sided inputs. J Theor Biol 18:300–315

Marcelis LFM, Heuvelink E, Goudriaan J (1998) Modelling biomass production and yield of horticultural crops: A review. Sci Hortic 74:83–111

Marchiori PE, Machado EC, Ribeiro RV (2014) Photosynthetic limitations imposed by self-shading in field-grown sugarcane varieties. Field Crops Res 155:30–37

Monsi M, Saeki T (1953) The light factor in plant communities and its significance for dry matter production. J Bot 14:22–52

Monteith JL (1965) Light distribution and photosynthesis in field crops. Ann Bot 29:17–37

Moriondo M, Leolini L, Staglianò N, Argenti G, Trombi G, Brilli L, Bindi M (2016) Use of digital images to disclose canopy architecture in olive tree.

Sci Hortic 209:1–13

Nederhoff EM, Vegter GJ (1994) Photosynthesis of stands of tomato, cucumber, and sweet pepper measured in greenhouses under various CO_2 concentrations. Ann Bot 73:353–361

Paulus S, Schumann H, Kuhlmann H, Léon J (2014) High-precision laser scanning system for capturing 3D plant architecture and analyzing growth of cereal plants. Biosyst Eng 121:1–11

Pearcy RW (1998) Acclimation to sun and shade: Photosynthesis. A Compre hensive Treatise. Cambridge Univ Press, Cambridge, UK, pp 250–263

Prusinkiewicz P (1986) Graphical applications of L-systems. Proc Graphics Interface 86:247–253

Qian T, Elings A, Dieleman JA, Gort G, Marcelis LFM (2012) Estimation of photosynthesis parameters for a modified Farquhar-von Caemmerer-Berry model using simultaneous estimation method and nonlinear mixed effects model. Environ Exp Bot 82:66–73

Room P, Hanan J, Prusinkiewicz P (1996) Virtual plants: New perspectives for ecologists, pathologists, and agricultural scientists. Trends Plant Sci 1:33–38

Sarlikioti V, de Visser PHB, Buck-Sorlin GH, Marcelis LFM (2011) How plant architecture affects light absorption and photosynthesis in tomato: Towards an ideotype for plant architecture using a functional-structural plant model. Ann Bot 108:1065–1073

Shin JH, Park JS, Son JE (2014) Estimating the actual transpiration rate with compensated levels of accumulated radiation for the efficient irrigation of soilless cultures of paprika plants. Agr Water Mgt 135:9–18

Sievänen R, Nikinmaa E, Nygren P, Ozier-Lafontaine H, Perttunen J, Hakula H (2000) Components of functional-structural tree models. Ann For Sci 57:399–412

Smith AR (1984) Plants, fractals, and formal languages. ACM SIGGRAPH Computer Graphics 18:1–10

Son JE, Park JS, Park HY (1999) Analysis of carbon dioxide changes in urban-type plant factory system. Hortic Environ Biotechnol 40:205–208

Suzaki T, Kume A, Ino Y (2003) Evaluation of direct and diffuse radiation densities under forest canopies and validation of the light diffusion effect. J For Res Jpn 8:283–290

Tanaka A, Kawano K (1966) Effect of mutual shading on dry-matter production in the tropical rice plant. Plant Soil 24:128–144

Thornley JHM (1976) Mathematical models in plant physiology. Academic Press Inc. Ltd. London, UK, p 318

Thornley JHM (1983) Crop yield and planting density. Ann Bot 52:257–259

Utsugi H (1999) Angle distribution of foliage in individual *Chamaecyparis obtusa* canopies and effect of angle on diffuse light penetration. Trees 14:1–9

Van Ittersum MK, Leffelaar PA, Van Keulen H, Kropff MJ, Bastiaans L, Goudriaan J (2003) On approaches and applications of the Wageningen crop models. Eur J Agron 18:201–234

Vos J, Marcelis LFM, Evers JB (2007) Functional-structural plant modelling in crop production: adding a dimension. Frontis 22:1–129

Wahabzada M, Paulus S, Kersting K, Mahlein AK (2015) Automated interpretation of 3D laser scanned point clouds for plant organ segmentation. BMC Bioinformatics 16:248

Wittwer SH, Robb WM (1964) Carbon dioxide enrichment of greenhouse atmospheres for food crop production. Econ Bot 18:34–56

Zhang Y, Teng P, Shimizu Y, Hosoi F, Omasa K (2016) Estimating 3D leaf and stem shape of nursery paprika plants by a novel multi-camera photography system. Sensors 16:874

APPENDICES

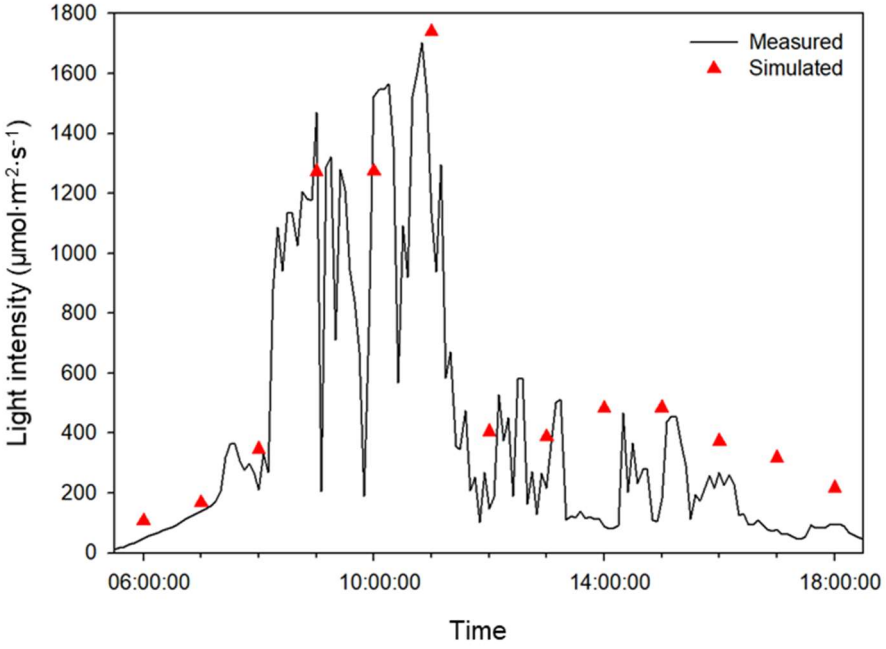

Fig. A1. Comparison of measured and simulated daily light intensity in a greenhouse (35.2ºN, 128.4ºE; Haman, Korea) on July 4, 2018.

Table A1. Plant height, number of leaves, and leaf area of 3D-scanned paprika plant at 7, 35, 63, 91, and 112 days after transplanting (DAT).

Growth stage (DAT)	Plant height (cm)	No. of leaves	Leaf area (m^2)
7	39.3	13	0.10
35	61.4	31	0.37
63	89.8	51	0.66
91	119.5	64	0.85
112	170.2	79	1.13

Table A2. Shading distance at the bottom of 3D paprika model at 7, 35, 63, 91, and 112 days after transplanting (DAT) at a solar altitude of 76.4º (12:00).

Growth stage (DAT)	Plant height (cm)	Shading distance (cm)
7	39.3	9.5
35	61.4	14.9
63	89.8	21.7
91	119.5	28.9
112	170.2	41.2

ABSTRACT IN KOREAN

온실에서는 높은 단위 생산성을 위해 높은 재식 밀도로 작물을 재배한다. 그러나 높은 재식 밀도 조건에서는 인접한 개체에 의한 상호 차광이 발생하여 캐노피 수광과 광합성을 감소시키고, 결과적으로 작물 수량과 품질의 저하를 초래한다. 이에 따라 최적 재식 밀도를 찾기 위한 연구가 진행되었으나, 이를 간접적인 단위로 표현하여 작물 간의 상호 작용에 대한 분석이 어렵다. 따라서 본 연구의 목적은 3차원 스캔 모델과 광학 시뮬레이션을 이용하여 파프리카의 생육 단계와 차광 조건에 따른 수광과 광합성 속도를 분석하는 것이다. 3차원 스캐닝을 통해 정식 후 7, 35, 63, 91, 112일의 작물 모델을 구축하였다. 작물의 차광 효과를 분석하기 위해 작물 모델을 60cm 간격으로 1 × 1, 3 × 3, 5 × 5, 7 × 7, 9 × 9로 정방형 배치하여 생육 단계별 시뮬레이션을 진행하였고, 중심에 위치한 개체의 수광량을 계산하였다. 캐노피 광합성 속도는 FvCB 모델을 이용하여 계산하였다. 시뮬레이션 결과 모든 생육 단계에서 주변 개체 수가 증가할수록 작물 수광량은 감소하였다. 특히, 단위 엽면적당 수광량은 작물의 생육이 진행됨에 따라 감소하였다. 이는 각 작물의 생육에 따른 자기 광 차단과 주변 작물의 증가에 따른

상호 광 차단 효과 때문으로 생각된다. 이산화탄소 소모량은 총 수광량과 비슷한 변화 양상을 보였으나, 작물 상단부에서 광합성 포화가 나타났기 때문에 수광량 변화에 감소율은 작았다. 본 실험에서는 파프리카의 3차원 스캔 모델과 광학 시뮬레이션을 이용하여 생육 단계와 주변 개체의 증감에 따른 작물의 수광과 광합성 변화를 분석할 수 있었다. 이는 추후 온실 내에서 작물 재배 시스템을 디자인하고, 수광과 광합성을 예측하는 데에 효과적인 방법이 될 수 있을 것이다.

주요어: 광 분포, 광 추적, 상호 광 차단, 자기 광 차단, 캐노피

학 번: 2017-28139